J Mater Sci (2008) 43:5564–5568
DOI 10.1007/s10853-008-2819-3

# Far infrared reflectance of sintered $Zn_2TiO_4$

**M. V. Nikolić · N. Obradović · K. M. Paraskevopoulos · T. T. Zorba · S. M. Savić · M. M. Ristić**

Received: 4 February 2008 / Accepted: 18 June 2008 / Published online: 8 July 2008


**Abstract** Zinc-titanate ceramics were obtained by initial mechanical activation in a high-energy planetary mill for 15 min followed by sintering at temperatures 900–1100 °C for 2 h. Room temperature far infrared reflectivity spectra for all samples were measured in the range 100–1200 $cm^{-1}$. The same ionic oscillators were present in the measured spectra, but their intensities increased with the sintering temperature in correlation with the increase in sample density and microstructure changes. Optical parameters were determined for seven oscillators belonging to the spinel structure using the four-parameter model of coupled oscillators. Born effective charges were calculated from the transversal/longitudinal splitting.

## Introduction

Zinc-titanate ($Zn_2TiO_4$) belongs to the group of "4-2" cubic oxide spinels ("4-2" denoting the combination of valence cations) that in bulk form is stable in the inverse spinel structure with $Zn^{2+}$ ions occupying tetrahedral voids and $Zn^{2+}$ and $Ti^{4+}$ ions randomly occupying octahedral voids [1, 2]. It has a face centered cubic unit cell, space group $Fd\bar{3}m$, with 8 formula units per cell, each consisting of 32 anions and 24 cations making a total of 56 atoms [3].

Zinc-titanate has been used as a catalyst and pigment [4–6]. As a catalyst, it has been used as a desulfurization sorbent for coal gasification of product gases. Zinc-titanate was also used as a component in dielectric compositions. Possible use of zinc-titanate as a photoluminescent material was studied in [7].

It is well-known that spinel structures can accommodate a certain degree of disorder described by the cation inversion parameter and also large deviations from stoichiometry. Far infrared reflection spectroscopy can enable a more clear insight into these complex structures. Thus, Lutz et al. [8] conducted a detailed analysis of lattice vibration spectra of a number of spinel type ternary oxides, while $MgAl_2O_4$ has been analyzed experimentally and theoretically using the density functional theory [9, 10]. Changes in far infrared reflection spectra as a result of different sintering times and temperatures of obtaining $NiMn_2O_4$ were analyzed in [11]. As far as cubic "4-2" spinels are concerned, far infrared reflectivity of $Zn_2SnO_4$ in bulk and thin film form was analyzed in [12, 13]. Chaves et al. [7] recorded IR spectra of $Zn_2TiO_4$ in the 400–4000 $cm^{-1}$ range.

In this work we have studied infrared optical reflectivity of $Zn_2TiO_4$ obtained by sintering in the temperature range 900–1100 °C for 2 h.

## Experimental

Zinc-titanate samples were prepared from ZnO (Aldrich, 99.99% p.a.) and $TiO_2$ (Aldrich, 99.99% p.a.) powders. The starting powders were mixed in ethanol with a magnetic whisk for 2 h and then dried at 120 °C for 2 h. The

M. V. Nikolić (✉)
Institute for Multidisciplinary Research, Kneza Višeslava 1, Belgrade 11000, Serbia
e-mail: maria@mi.sanu.ac.yu; mariavesna@cms.bg.ac.yu

N. Obradović · S. M. Savić · M. M. Ristić
Institute of Technical Sciences of SASA, Knez Mihailova 35/IV, Belgrade 11000, Serbia

K. M. Paraskevopoulos · T. T. Zorba
Department of Physics, Solid State Section, Aristotle University, Thessaloniki, Greece

powders were then mechanically activated for 15 min in a planetary ball mill (Fritch Pulversette 5). The resulting powders were sieved through a 0.22 mm sieve and then compacted with a pressure of 4 t/cm$^2$ into discs 8 mm in diameter. The compacts obtained were sintered non-isothermally to 900–1100 °C and then held at those temperatures for 2 h. Sample density was calculated from measurements of the sample diameter, thickness, and mass.

X-ray diffraction (XRD) patterns of the sintered samples were measured on a Philips PW 1050 diffractometer with $\lambda CuK_\alpha$ radiation (step 0.05 s). Structural refinement was carried out by the Rietveld method using the GSAS package [14] with the EXPGUI graphical user interface [15]. $Zn_2TiO_4$ cubic spinel was refined with space group $Fd\bar{3}m$ (origin $\bar{3}m$) assuming a degree of inversion of 1, with $Zn^{2+}$ cations on 8a and 16d sites and $Ti^{4+}$ cations on 16d sites and O occupying site 32e. Initial cell and position parameters and also isotropic temperature parameters were taken from Millard et al. [2]. All sites were assumed to be fully occupied. Variations of both $Zn_2TiO_4$ stoichiometry and site occupancy were undertaken during Rietveld refinement of XRD data, but they did not change significantly the determined values of the cell parameters, so we assumed that the cation inversion parameter was 1 and that the spinel was stoichiometric within error. As ZnO is the extra phase possibly present in most $Zn_2TiO_4$ samples, it was refined in the space group $P6_3mc$ using initial cell parameters, position parameters, and temperature parameters from Abrahams and Berstein [16]. The morphology of sintered samples was analyzed by scanning electron microscopy (SEM) on a JSM-6460LV JEOL 25 kV device.

Room temperature infrared optical reflectivity measurements were performed with near normal incidence light in the range between 100 and 1200 cm$^{-1}$ using a Bruker 113 V FTIR spectrometer, with measurements resolution higher than 1 cm$^{-1}$. All samples were highly polished before the measurements using silicon carbide sand paper (P1000 and P1500) and finally 3 μm grade diamond paste to obtain a surface suitable for reflectivity measurements.

## Results and discussion

XRD analysis of the samples sintered at 900, 1000, and 1100 °C shows that an almost pure $Zn_2TiO_4$ phase is present. Very small peaks for ZnO are noticeable in the XRD pattern obtained for samples sintered at 900 °C (Fig. 1a) but they are not noticeably present in the samples sintered at 1100 °C (Fig. 1b). The results of refinements of XRD patterns are given in Table 1. The amount of ZnO phase was in the range 0.6–2 wt.% and it was lower for higher sintering temperatures. Similar amounts of excess ZnO (1–3%) were found in $Zn_2TiO_4$ by Millard et al. [2].

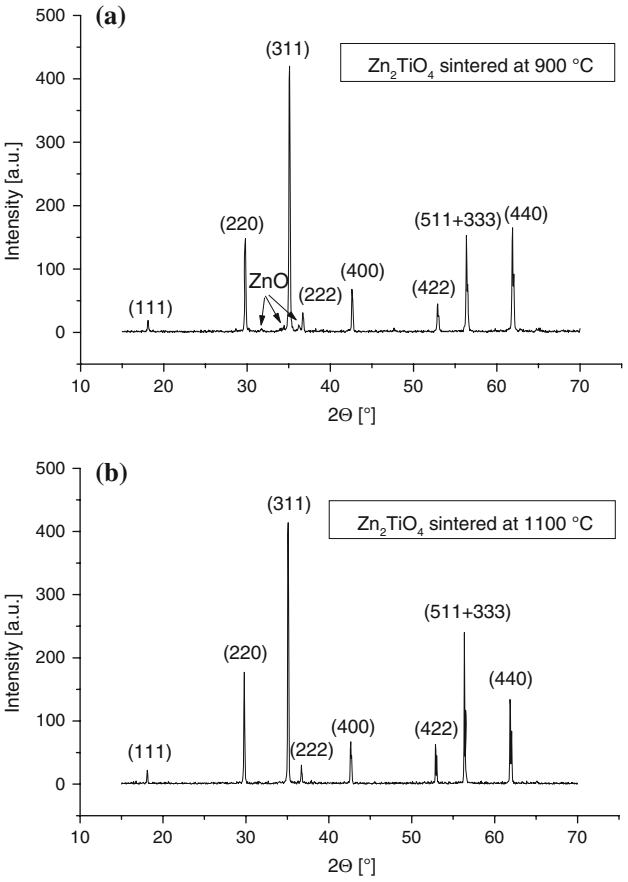


**Fig. 1** X-ray diffraction pattern for $Zn_2TiO_4$ sintered at 900 °C (**a**) and 1100 °C (**b**)

**Table 1** Structural parameters of $Zn_2TiO_4$ sintered in the range 900–1100 °C

| $T$ (°C) | $a$ (Å) | $u$ | $Zn_2TiO_4$ (wt.%) | ZnO (wt.%) |
|---|---|---|---|---|
| 1100 | 8.47328 | 0.259 | 99.35 | 0.65 |
| 1000 | 8.47172 | 0.258 | 98.87 | 1.13 |
| 900 | 8.47145 | 0.257 | 98.03 | 1.97 |

The average green sample density was 67.52% of the theoretical density. The sample density increased with increasing sintering temperature giving 3.591 g/cm$^3$ at 900 °C, 4.048 g/cm$^3$ at 1000 °C, and 4.586 g/cm$^3$ at 1100 °C representing 70.97, 80, and 90.63% of the theoretical density (5.060 g/cm$^3$). Changes in the microstructure of $Zn_2TiO_4$ samples for different sintering temperatures are shown in Fig. 2. At 900 °C (Fig. 2a) the presence of porosity is noticeable in the samples and the sintering process is in the intermediate stage, while the sintering process has advanced further at 1000 °C and the porosity is lower (Fig. 2b); this is in correlation with changes in the sample density.

The reflectivity of $Zn_2TiO_4$ samples sintered at different temperatures is given in Fig. 3. One can note the presence

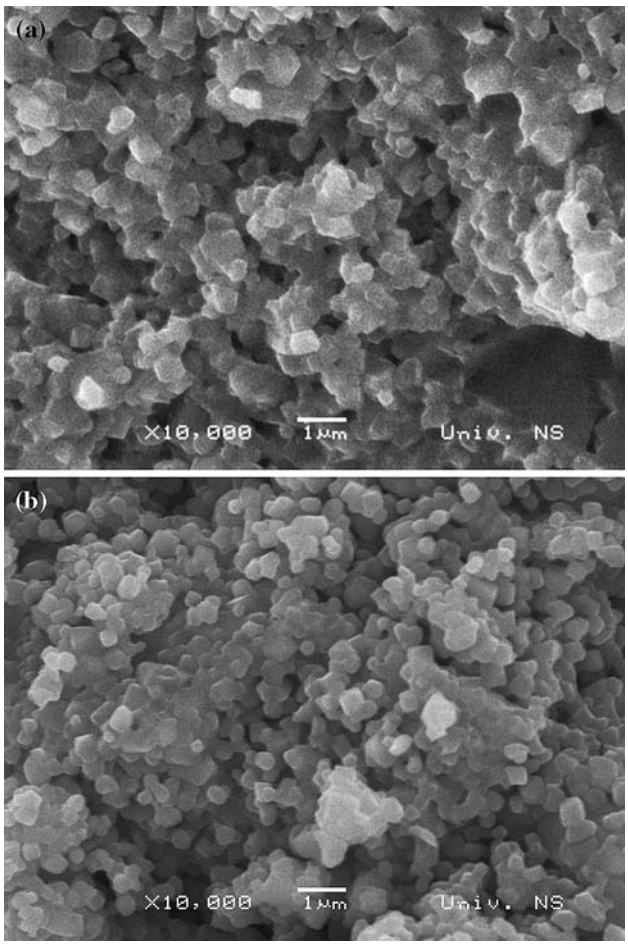


**Fig. 2** Microstructure of $Zn_2TiO_4$ sintered at 900 °C (**a**) and 1000 °C (**b**)

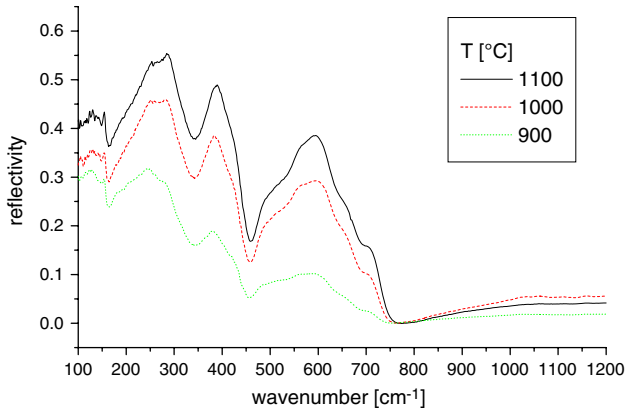


**Fig. 3** Reflectivity spectra of $Zn_2TiO_4$

of the same peaks, but the peak intensity increased with the sample density, i.e., sintering temperature. The peaks at lower sintering temperature were also broader. Thus, for $Zn_2TiO_4$ four expressed peaks can be noted, with two to three possible shoulders.

**Table 2** Transversal and longitudinal modes and corresponding damping factors (all in $cm^{-1}$) and the high frequency dielectric permittivity obtained for $Zn_2TiO_4$ samples sintered at 900 °C (ZTI09), 1000 °C (ZTI10), and 1100 °C (ZTI11) for 2 h

| Oscillator | Parameter | Sample | | |
|---|---|---|---|---|
| | | ZTI09 | ZTI10 | ZTI11 |
| | $\varepsilon_\infty$ | 1.8 | 3.2 | 2.9 |
| I | $\omega_{TO}$ | 158.9 | 158.9 | 158.9 |
| | $\gamma_{TO}$ | 58.2 | 30.7 | 38.6 |
| | $\omega_{LO}$ | 160.3 | 160.3 | 160.3 |
| | $\gamma_{LO}$ | 36.0 | 23.2 | 24.6 |
| II | $\omega_{TO}$ | 160.5 | 160.5 | 160.5 |
| | $\gamma_{TO}$ | 196.8 | 345.0 | 102.4 |
| | $\omega_{LO}$ | 187.4 | 187.4 | 187.4 |
| | $\gamma_{LO}$ | 592.9 | 334.9 | 168.6 |
| III | $\omega_{TO}$ | 259.3 | 259.3 | 259.3 |
| | $\gamma_{TO}$ | 408.4 | 100.6 | 84.3 |
| | $\omega_{LO}$ | 326.9 | 326.9 | 326.9 |
| | $\gamma_{LO}$ | 74.6 | 69.7 | 79.7 |
| IV | $\omega_{TO}$ | 355.7 | 366.0 | 371.8 |
| | $\gamma_{TO}$ | 94.1 | 77.4 | 77.4 |
| | $\omega_{LO}$ | 424.9 | 451.9 | 444.0 |
| | $\gamma_{LO}$ | 66.4 | 71.4 | 64.7 |
| V | $\omega_{TO}$ | 494.0 | 483.1 | 488.8 |
| | $\gamma_{TO}$ | 189.6 | 42.3 | 47.6 |
| | $\omega_{LO}$ | 494.7 | 488.0 | 498.3 |
| | $\gamma_{LO}$ | 33.1 | 80.6 | 64.1 |
| VI | $\omega_{TO}$ | 577.2 | 555.0 | 541.5 |
| | $\gamma_{TO}$ | 74.0 | 108.4 | 111.7 |
| | $\omega_{LO}$ | 600.3 | 650.8 | 659.5 |
| | $\gamma_{LO}$ | 438.0 | 135.1 | 116.2 |
| VII | $\omega_{TO}$ | 720.6 | 720.6 | 720.6 |
| | $\gamma_{TO}$ | 319.8 | 141.1 | 116.8 |
| | $\omega_{LO}$ | 723.3 | 723.3 | 723.3 |
| | $\gamma_{LO}$ | 146.7 | 44.6 | 32.9 |

Analysis of the measured spectra was performed using the four-parameter model of coupled oscillators [17]:

$$\varepsilon = \varepsilon_1 + i\varepsilon_2 = \varepsilon_\infty \prod_j \frac{\omega_{jLO}^2 - \omega^2 + i\gamma_{jLO}\omega}{\omega_{jTO}^2 - \omega^2 + i\gamma_{jTO}\omega} \quad (1)$$

where $\omega_{jTO}$ and $\omega_{jLO}$ are transverse (TO) and longitudinal (LO) frequencies, $\gamma_{jTO}$ and $\gamma_{jLO}$ are TO and LO damping factors, respectively, while $\varepsilon_\infty$ is the high frequency dielectric permittivity. Seven vibration modes were determined for all samples and the values of all calculated optical parameters are given in Table 2 and an example of the good agreement between the measured and calculated is shown in Fig. 4 for $Zn_2TiO_4$ sintered at 1100 °C. One

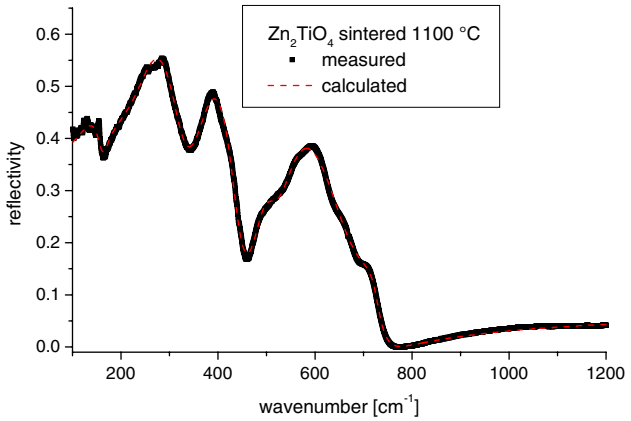


**Fig. 4** Measured (full line) and calculated (dotted line) reflectivity spectra of $Zn_2TiO_4$ sintered at 1100 °C

can see that with the increase in the sintering temperature oscillators I, II, III, and VII differ only in damping factors, while the values of the transversal and longitudinal modes are the same. For the other three oscillators, transversal and longitudinal mode positions differ very slightly. Four of the determined modes were below the range recorded by Chaves et al. [7]. The last three modes are at similar positions.

Born effective charges can be calculated from TO/LO splittings of the phonon modes using the relation [18]:

$$\sum_{j=1}^{n_{\mathrm{IR}}} \left(\omega_{j\mathrm{LO}}^2 - \omega_{j\mathrm{TO}}^2\right)_a = \frac{1}{\varepsilon_0 V} \sum_{k=1}^{n_{\mathrm{atom}}} \frac{Z_{ka}^2 e^2}{m_k} \tag{2}$$

where $a$ is the polarization direction, the summation on the right-hand side of the equation is over all atoms in the unit cell and the summation on the left-hand side is over all active IR-modes, $\varepsilon_0$ is the vacuum dielectric constant, $V$ is the unit cell volume, $m_k$ is the atomic mass and $e$ is the electron charge. The charge neutrality condition also needs to be satisfied and in the case of $Zn_2TiO_4$ it is:

$$Z_{\mathrm{Ti}} + 2Z_{\mathrm{Zn}} + 4Z_{\mathrm{O}} = 0 \tag{3}$$

where $Z_{\mathrm{Ti}}$, $Z_{\mathrm{Zn}}$, and $Z_{\mathrm{O}}$ are the Born effective charges of Ti, Zn, and O atoms. In the ideal case these charges would be +4 for Ti, +2 for Zn, and −2 for O atoms. Using equations (2) and (3) the Born effective charges were calculated as: $Z_{\mathrm{O}} = 1.970$, $Z_{\mathrm{Zn}} = 1.979$, and $Z_{\mathrm{Ti}} = 3.922$. These values are slightly lower than the formal charges of these cations, indicating some hybridization between the cations and O anions due to structural disorder and defects.

As the space group determined for $Zn_2TiO_4$ is $Fd\bar{3}m$, with 8 formula units per cell, each consisting of 32 anions and 24 cations making a total of 56 atoms, the total number of active and inactive IR and Raman modes can be calculated using nuclear site group analysis [19]:

$$\Gamma = A_{1\mathrm{g}}(\mathrm{R}) + E_{\mathrm{g}}(\mathrm{R}) + 3F_{2\mathrm{g}}(\mathrm{R}) + 4F_{1\mathrm{u}}(\mathrm{IR}) + F_{1\mathrm{g}} + 2A_{2\mathrm{u}} + 2E_{\mathrm{u}} + 2F_{2\mathrm{u}}$$

where R denotes Raman activity and IR denotes infrared activity, the fifth $F_{1u}$ IR mode is an acoustic mode and the remaining modes are silent. Thus, theory predicts four modes for normal spinel structures. We calculated seven for $Zn_2TiO_4$ in the inverse spinel structure. If we observe the measured spectra in Fig. 3, we can note that there are four peaks, but the first one is calculated as two modes and the fourth-last one as three modes (the two shoulders are quite visible). Literature data [8–13] shows that more peaks than the theoretically predicted number has been determined for many analyzed spinel oxide structures, including "4-2" inverse spinel $Zn_2SnO_4$ [12, 13]. Structural disorder can be one of the reasons. Some extra vibrations could be due to cation exchange, as in the case of $MgAl_2O_4$ [9]. Zinc also has a high vapor pressure, so zinc-vacancies can form leading to deviations from stoichiometry.

Millard et al. [2] determined by Rietveld refinement that cubic $Zn_2TiO_4$ was almost completely inverse (inversion degree at 1210 °C was 99.8%) with space group $Fd\bar{3}m$and calculated the lattice constant as $a = 8.46948$ Å and anion displacement parameter $u = 0.2606$ and bond lengths as T–O = 1.989 and M–O = 2.032 Å, for mostly $Zn^{2+}$ ions and a very small number of $Ti^{4+}$ ions on tetrahedral sites and $Zn^{2+}$ and $Ti^{4+}$ ions on octahedral sites, respectively. The value of the anion displacement parameter has a value higher than the ideal one for a perfect fcc lattice ($u = 0.250$, origin at $\bar{3}m$) resulting in increased tetrahedral bond lengths and decreased octahedral bond lengths (whose ideal ratio is M–O/T–O = 1.155 [1]). The values obtained in this work given in Table 1 are similar. For the lattice constant they are slightly higher and the anion displacement parameter values are slightly lower. Zn atoms have shallow occupied valence $d$ states and prefer to occupy the tetrehedral sites making $Zn_2TiO_4$ stable in the inverse spinel structure with ½ $Zn^{2+}$ ions on tetrahedral sites and the cation inversion parameter very close to 1. In this work we assumed it to be 1, as variations of both $Zn_2TiO_4$ stoichiometry and site occupancy were attempted during Rietveld refinement of XRD data, but they did not change significantly the values of the cell parameters given in Table 1. In the inverse spinel structure, $Zn^{2+}$ and $Ti^{4+}$ ions randomly occupy octahedral sites and the long-range symmetry of the structure is broken. The presence of excess $Zn^{2+}$ ions was noted in stoichiometric spinel $ZnCr_2O_4$ due to solution of small amounts of ZnO in the spinel lattice [20]. The excess $Zn^{2+}$ ions can be distributed on tetrahedral and octahedral sites and vacancies are created to compensate. Wang et al. [21] studied Raman spectra of $Zn_2TiO_4$ and found that even though the

observed number of modes matched the theoretically predicted number, the background was high and the characteristics were broad indicating a large ratio of disorder in the analyzed sample. Thus, defects and disorder can be the reason for the higher number of calculated modes compared to the theoretically predicted number. One should emphasize that these modes reflect complex vibrations in the crystal lattice including all atoms in it [8]. Infrared reflection measurements at low temperatures could contribute to explaining the origin of the additional vibration modes accompanied by calculations based on the density functional theory.

## Conclusion

$Zn_2TiO_4$ was obtained by sintering mechanically activated (15 min) powder mixtures of ZnO and $TiO_2$ at temperatures from 900 to 1100 °C. XRD analysis showed that an almost pure $Zn_2TiO_4$ phase (containing 0.6 wt.% ZnO) was obtained at 1100 °C, while noticeable traces of ZnO were present in samples sintered at 1000 and 900 °C, namely 1.13 and 1.97 wt.%. Room temperature infrared reflection spectra were measured and analyzed. Seven oscillators belonging to the spinel structure were calculated and discussed in relation to the four theoretically predicted for normal spinel structures. The extra three oscillators originate from the disorder due to cation inversion in inverse spinel structures and defects due to the presence of low amounts of ZnO in samples. Born effective charges were calculated for $Zn_2TiO_4$ sintered at 1100 °C s: $Z_O = 1.970$, $Z_{Zn} = 1.979$, and $Z_{Ti} = 3.922$ showing that some hybridization exists between Zn and Ti cations and O anions, though its effect is weak.

**Acknowledgements** The authors would like to express their gratitude to Dr. M. Mitric for X-ray measurements. This work was partially financed by the Ministry for Science of the Republic of Serbia through project 142011G and F 7/2 financed by the Serbian Academy of Sciences and Arts.

## References

1. Hill RJ, Craig JR, Gibbs GV (1979) Phys Chem Miner 4:317
2. Millard RL, Peterson RC, Hunter BK (1995) Am Mineral 80:885
3. Sickafus KE, Wills JM, Grimes NW (1999) J Am Ceram Soc 82:3279
4. Lysova NN, Shapavalova LP, Luk'yanenko VP (1991) Inorg Mater 27:542
5. Walton KS, Datta RK (1995) Ceram Trans 61:637
6. Mikhailov MM, Dvoretskii MI (1991) Inorg Mater 27:2021
7. Chaves AC, Lima SJG, Araujo RCMU, Maurera MAMA, Longo E, Pizani PS, Simoes LGP, Soledade LEB, Souyz AG, dos Santos IMG (2006) J Solid State Chem 179:985
8. Lutz HD, Muller B, Steiner HJ (1991) J Solid State Chem 90:54
9. Thibaudeau P, Gervais F (2002) J Phys Condens Matter 14:3543
10. Bi C-Z, Ma J-Y, Yan J, Zhao B-R, Yoo D-Z, Qiu X-G (2006) Chin Phys 15:1090
11. Nikolic MV, Paraskevopoulos KM, Aleksic OS, Zorba TT, Savic SM, Blagojevic VD, Lukovic DT, Nikolic PM (2007) Mater Res Bull 42:1492
12. Nikolic MV, Ivetic T, Paraskevopoulos KM, Zorbas KT, Blagojevic V, Vasiljevic-Radovic D (2007) J Eur Ceram Soc 27:3727
13. Nikolic MV, Ivetic T, Young DL, Paraskevopoulos KM, Zorba TT, Blagojevic V, Nikolic PM, Vasiljevic-Radovic D, Ristic MM (2007) Mater Sci Eng B 138:7
14. Larson A C, Von Dreele R B (2004) General Structure Analysis System (GSAS) Los Alamos National Laboratory Report LAUR 86-748
15. Toby BH (2001) J Appl Cryst 34:210
16. Abrahams SC, Berstein JL (1969) Acta Crystallogr B25:1233
17. Gervais F, Piriou B (1974) Phys Rev B 10:1642
18. Kurosawa T (1961) J Phys Soc Jpn 16:1298
19. Rousseau DL, Bauman RP, Porto SPS (1981) J Raman Spectrosc 10:253
20. Grimes RW, Binks DJ, Lidiard AB (1995) Phil Mag A 72:651
21. Wang Z, Saxena SK, Zha CS (2002) Phys Rev B 66:024103